INTERNATIONAL JOURNAL OF HYDROGEN ENERGY 33 (2008) 3351–3367

Available at www.sciencedirect.com

ScienceDirect

journal homepage: www.elsevier.com/locate/he

Investigation of macro- and micro-porous layer interaction in polymer electrolyte fuel cells

Ramaraja P. Ramasamy[a], *Emin C. Kumbur*[a], *Matthew M. Mench*[a,*], *Wen Liu*[b], *Deborah Moore*[b], *Mahesh Murthy*[b]

[a]*Department of Mechanical and Nuclear Engineering, Fuel Cell Dynamics and Diagnostics Laboratory, The Pennsylvania State University, University Park, PA 16802, USA*

[b]*Gore Fuel Cell Technologies, W. L. Gore & Associates Inc., Elkton, MD 21921, USA*

ARTICLE INFO

Article history:
Received 3 December 2007
Received in revised form
8 March 2008
Accepted 15 March 2008
Available online 9 June 2008

Keywords:
Capillary transport
Gas diffusion layer
Flooding
Micro-porous layer
Two-phase transport
Water management

ABSTRACT

An array of carefully selected commercial diffusion media (DM) in combination with different micro-porous layers (MPLs) were subjected to extensive performance testing over a wide range of operating conditions to delineate the effects of DM–MPL configuration on the cell performance. Along with *in situ* and *ex situ* AC impedance measurements, durability tests were also performed to isolate the corresponding ohmic and mass transfer characteristics under wet and dry conditions, and to probe the degradation in the internal structure of these sub-layers under short- and long-term operations. Results indicate the existence of a strong and complex interaction between the macro- and micro-porous layers of the gas diffusion electrode. However, the nature of this interaction does not follow any obvious trend with respect to the bulk properties of the tested DM materials, indicating that the multi-phase transport cannot be described solely through a capillary transport concept (i.e. pore size, porosity and hydrophobicity). In addition, the hydrophobic treatment of the DM is found to be beneficial to alleviate flooding under wet conditions, but this beneficial effect gradually diminishes as the operating conditions become drier. The presence of an MPL appears to mitigate the loss of hydrophobicity in the macro-porous DM under long-term operations. Finally, the interaction between the membrane and the DM is found to be considerably different on both electrodes, indicating that a half cell modeling approach considering only a single electrode would lead to less realistic predictions.

1. Introduction

The fuel cell diffusion media (DM) is a specially engineered porous media that provides a critical link between the electrochemical activity and the micro-fluidic management of a polymer electrolyte fuel cell (PEFC). Because of the vital role of this component, enhancing the performance of PEFCs through engineering this porous material is the subject of a large number of experimental [1–9] and modeling studies [10–28]. Ideally, the porous fuel cell DM serves to provide a uniform distribution of the reactants in the electrodes, while ensuring proper and rapid transport of product water and electrons, as well as removal of excess heat. In particular, the role of DM in the water management is critical, since significant improvement in PEFC performance can be directly linked to the minimization of the mass and ohmic transport losses occurring in the porous electrodes [29–33].

*Corresponding author. Tel.: +1 814 865 0060; fax: +1 814 863 4848.
E-mail address: mmm124@psu.edu (M.M. Mench).
0360-3199/$ - see front matter © 2008 International Association for Hydrogen Energy. Published by Elsevier Ltd. All rights reserved.
doi:10.1016/j.ijhydene.2008.03.053

Typically, the porous DM is constructed from a sheet of electrically conductive macro-porous substrate, such as a non-woven carbon paper or a woven carbon cloth. Both non-woven carbon paper and woven-cloth DM have complex and heterogeneous structure with pore size ranging from a few microns to tens of microns. In terms of water management, the degree of wettability in the pore structure governs the water retention in the DM, influencing the amount of liquid water imbibition and storage within the solid pore matrix [34]. The naturally hydrophilic porous substrates are typically impregnated with a non-uniform coating of hydrophobic agent known as Teflon® (polytetrafluoroethylene or PTFE) to achieve the desired wettability for effective water removal. Due to the heterogeneous nature of the PTFE coating, the DM internal pore structure exhibits a mixed wettability characteristic with multi-modal pore configuration [35], with different fractions of hydrophobic, hydrophilic pores and partially hydrophobic/hydrophilic (mixed) pores, as illustrated in Fig. 1.

In addition to the bulk hydrophobic treatment, an additional thin micro-porous layer (MPL) of carbon black mixed with PTFE is usually applied to the DM macro-substrate to provide better electrical contact and mechanical compatibility between the layers, and to reduce the cathode DM flooding [36–37]. The inclusion of an MPL between the DM and the CL on the cathode side aids in directing the liquid water flow to the anode side through the polymer membrane, thus impeding the dehydration of the membrane [36–37]. In addition, the MPL on the anode side can serve as a diffusion barrier, preventing membrane dehydration under low humidity conditions [13]. Another positive impact of adding a MPL is the prevention of DM fiber intrusion into the CL. Due to its critical role in improving water management, prior research efforts [38–41] have been focused on investigating the effect of physical properties of the MPL (i.e., carbon black, hydrophobic agent, thickness, etc.) on fuel cell performance. These efforts were primarily targeted to determine the optimum internal architecture of the MPL, without considering the interfacial effects at the MPL and macro-DM backing layer.

Considering the various roles of the DM, it is very challenging to establish a precise link between the myriad material properties of the bi-layered DM and the fuel cell performance. To date, most studies underline the significance of the need for gaining a more refined understanding of transport mechanism and the role of DM and MPL morphology on the long- and short-term cell performance. Even when the internal structure of the DM and MPL were analyzed, different pore morphology was observed to yield significant variations in the micro-scale phase distributions inside the DM and flow channel [34]. Therefore, establishing effective micro-fluidic management in an operating PEFC requires a detailed knowledge of underlying physics of the complex microscopic transport phenomena within the porous electrodes. This involves a number of material-dependent parameters, including carbon loading, pore morphology, mass transport resistance, wettability characteristics (PTFE loading), and most importantly the interaction between the sub-layers (i.e., micro- and macro-substrates) of the porous DM. Based on this motivation, significant efforts have been focused on establishing structure–property–performance relationships [38–42], and the advantages of inclusion of the MPL to base DM substrates are repeatedly expressed in the literature. However, the exact nature of the interaction between the macro-DM backing layer and the MPL has not been conclusively addressed beyond basic capillary flow arguments, and remains a subject of debate.

This study is motivated by the need to understand the underlying interactions between the sub-layers (MPL and

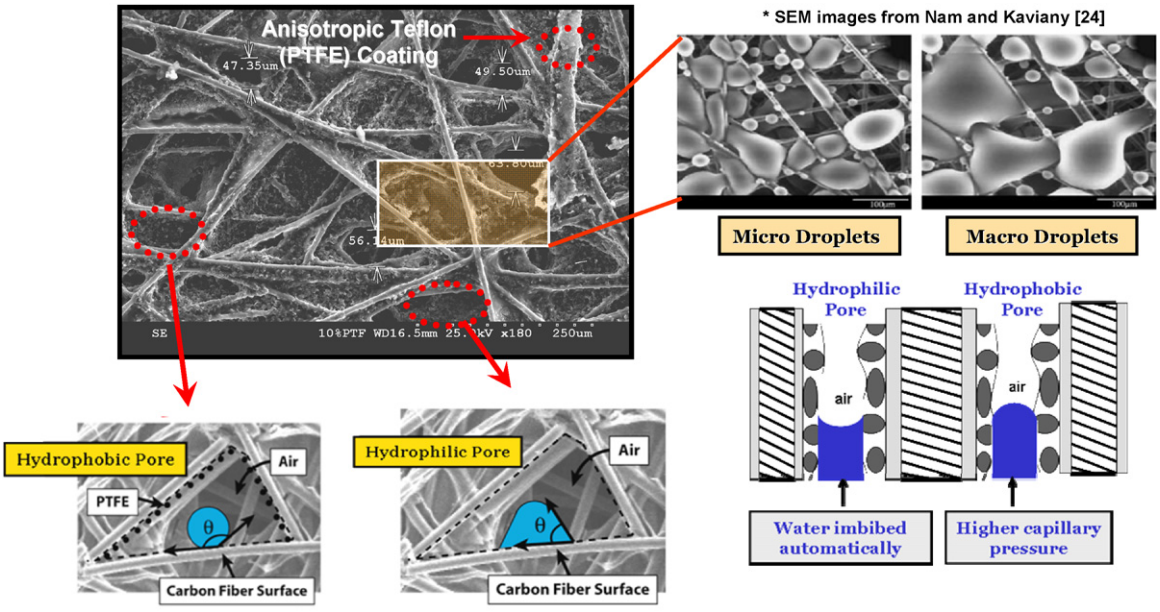

Fig. 1 – SEM images showing the dual pore network characteristic of a fuel cell DM and schematic of liquid water behavior in hydrophobic and hydrophilic pores of DM.

macro-DM substrates) of the porous fuel cell DM. Different types of commercially available DM samples (with or without MPL) were subjected to extensive testing under a wide range of operating conditions. Special experimental protocols were designed to delineate the effects of various DM–MPL configurations on the overall cell performance, and to probe the degradation in the internal structure of these sub-layers under short- and long-term operations. Along with the performance diagnostics, *in situ* and *ex situ* AC impedance testing were also performed to isolate the corresponding ohmic and mass transfer characteristics of the fuel cell that has different porous electrode configuration (i.e., DM with or without MPL) under wet and dry conditions.

2. Method of approach

2.1. Materials

Three types of carbon-fiber based fuel cell DM from different manufactures were examined in this study. The base DM macro-substrates utilized in the experiments are namely; Carbel carbon cloth (from W. L. Gore & Associates), TGP 060 carbon paper (from TORAY™) and SGL 31 and 10 series non-woven carbon paper DM (from SIGARET™ Carbon group). The chosen DM types exhibit different morphological structure (i.e., pore size, porosity, thickness, etc.), and are commonly used in fuel cell operation. The material properties of the bare DM substrates (without MPL) tested in this study are provided in Table 1.

Different combinations of macro-DM substrate and MPL were tested to examine the performance behavior of the fuel cell as a function of different DM combinations. Three main DM base substrates (specified above) were used in combination with two different types of MPL namely, Carbel® MP30z micro-layer and porous carbon/PTFE micro-layer, both supplied from W. L. Gore & Associates. The MP30z micro-layer has a thicker (~50–65 μm) and exclusively hydrophobic structure with an average pore size less than 0.1 μm. The carbon/PTFE micro-layer was composed of carbon–PTFE mixture (5% PTFE and 95% carbon), with a thinner structure (~20–30 μm).

2.2. Fuel cell specifications

Fuel cell tests were performed using a custom designed 25 cm^2 fuel cell. The cell consisted of two graphite bipolar end plates with a triple channel serpentine flow pattern. The bolt-loaded cell was assembled with uniform compression of ~830 kPa/bolt on the active area. Besides a set of silicon gaskets, additional polyethylene napthalate (PEN) sub-gaskets were also used to maintain a uniform compression on the cell active area, and to minimize the possible edge effects inside the fuel cell. Ultra high purity hydrogen and breathing quality air were utilized as the fuel and the oxidant in the fuel cell, respectively. In the experiments, Gore™ PRIMEA® 57 Series, 18 μm thick reinforced polymer electrolyte membranes coated with a platinum loading of 0.4 mg/cm^2 on each electrode were used.

In terms of porous backing-layer, Gore™ Carbel CL was used as the standard DM substrate on both anode and cathode sides, however in the comparison tests, this DM was replaced with Toray 060 (paper) or SGL 31BA (non-woven) on either anode or cathode side. As mentioned in previous section, the base DM materials used on the cathode electrode were coated either with an exclusively hydrophobic MP30z micro-layer on the catalyst layer or a partially hydrophobic carbon/PTFE coating on the macro-DM substrate.

2.3. Fuel cell testing and AC impedance measurements

2.3.1. Fuel cell testing

The fuel cell performance testing was performed with a Globe-Tech Gas Sub Unit test station, and a Scribner load unit model 890B. Polarization curves were recorded under both potentiostatic and galvanostatic conditions. MEAs were conditioned prior to the DM evaluation by operating the cells in fully humidified state with Gore™ Carbel CL DM on both anode and cathode sides. After the MEA was fully conditioned, the cathode or the anode DM was removed, and replaced with the macro DM–MPLs combination chosen for testing. The cell assembly was then preconditioned for another 30 min in order to ensure that the tested DM substrates achieved a precondition state.

Table 1 – Material properties of the tested bare macro-DM substrates (without MPL)

Material	Type	Thickness (μm)	Porosity	PTFE (% by wt)	Measured surface contact angle (deg)
Gore™ Carbel CL®	Carbon cloth	400	0.82	5	~145
Toray™ TGP 60®	Carbon paper	190	0.80	5	~120
Sigracet™ SGL 10BA®	Non-woven paper	420	0.88	5	~153
Sigracet™ SGL 31BA®	Non-woven paper	200	0.83	5	N/A

Table 2 – Test conditions for wet and dry cases

Operating condition	Wet case	Dry case
Cell temperature, °C	60	95
Inlet relative humidity (H_2/air), %	100/100	50/0
Outlet relative humidity[a] (Air), %	305	69
Back pressure (kPa)	270	270
Stoichiometric ratio (A/C)	1.2/2.0	1.2/2.0
Minimum inlet flow rate of hydrogen/air (cm^3/min)	50/100	50/100

[a] Calculated based on a mass balance of water in fuel cell cathode at 1 A/cm^2, and 100% inlet relative humidity, assuming no cross-over values >100% indicate condensation.

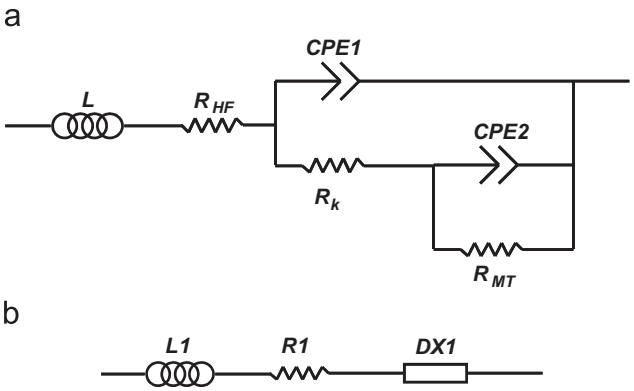

Fig. 2 – (a) Equivalent electrical circuit model used to fit *in situ* Nyquist data. *L*—inductance, R_{HF}—high frequency resistance, R_k—kinetic resistance, R_{MT}—mass transfer resistance, CPE1 and CPE2—constant phase elements; (b) equivalent circuit model to fit *ex situ* AC impedance data. L1—inductor, R1—resistor and DX1—transmission line circuit.

The polarization curves and AC impedance scans were recorded at two different operating scenarios, wet and dry. The specifications of the operating conditions in these two different scenarios are given in Table 2. For the wet condition, the cell temperature was kept at 60 °C, whereas the inlet anode and cathode relative humidity (RH) were maintained at 100%, respectively. For the dry condition, the cell temperature was kept at 95 °C; whereas the RH of the anode and cathode inlets were maintained at 50% and nearly 0%, respectively. For both conditions, the fuel and the oxidizer stoichiometric ratios were 1.2 and 2, with a minimum flow rate of 50 and 100 cm^3/min, respectively.

2.3.2. *AC impedance measurements*

Electrochemical impedance spectroscopy (EIS) was performed at various current densities ranging from 0.1 to 2.5 A/cm^2 with a Solatron™ SI 1280B frequency analyzer unit. To ensure steady state, the operating fuel cell was allowed to equilibrate at least 10 min before performing the impedance scans. For *in situ* AC impedance measurements, the oxygen electrode was used as the working electrode, whereas the hydrogen electrode was utilized as both counter and reference. A sinusoidal current signal was applied to the fuel cell and the amplitude of the AC current was continuously adjusted according to the fuel cell current to obtain the steady impedance measurements.

Ex situ high frequency resistance (HFR) measurements were also performed on the fully moist MEA that was exposed to fully humidified nitrogen at 60 °C in a specially designed test setup (a non-operational fuel cell test stand). The detailed procedure for *ex situ* AC impedance test is provided in Ref. [43]. During these measurements, six different inlet RH conditions ranging from 10% to 90% were tested, and the corresponding EIS spectra were obtained within the frequency range from 0.1 to 8000 Hz for these RH conditions. An equivalent electrical circuit fitting method was used to analyze and determine the MEA resistance (R_{MEA}), the DM resistance (R_{DM}), the kinetic resistance (R_k) and the mass transfer resistance (R_{MT}). The electrical circuit used for fitting the EIS data is shown in Fig. 2. The model circuit consists of an inductor, a resistor in the high frequency region, and two parallel RC circuits connected to each other in series. The inductor accounts for the influence associated with the external electrical connections. The parallel RC elements simulate the kinetic and mass transport behaviors. The capacitor in the RC circuit is modeled as a constant phase element (CPE) to account for the capacitive losses that generally occur in the porous electrode. The governing resistance parameters, such as R_{MT}, R_k and R_{HF} were evaluated using equivalent electrical circuit fitting of the Nyquist data method. A detailed description of extracting the MEA resistance and the mass transfer resistance using the equivalent circuit fitting method is provided in Appendix A.

3. Results and discussion

3.1. *Cathode DM–MPL configurations*

3.1.1. *Cathode performance under wet condition*

Under extremely wet conditions, the cathode tends to flood especially at high current densities. The porous DM exposed to the excess liquid water suffers from high mass transfer resistance R_{MT}, thereby significantly limiting the cell performance. The most favorable DM configuration is expected to yield the lowest mass transfer resistance (R_{MT}) over a wide range of current densities that would enable to alleviate the flooding effect, and thus provide the highest cell performance under wet conditions. Table 3 presents the tested DM configurations of three main sets (i.e., Carbel CL cloth, SGL 31BA and TGP 060) coated with different MPL materials (i.e., MP30z and carbon/PTFE micro-layer).

3.1.1.1. Cloth series. Fig. 3a compares the performance of all three configurations of Carbel CL cloth DM namely, C (bare Carbel CL), C+M (Carbel CL coated with MP30z micro-layer) and C+C (Carbel CL coated with carbon/PTFE micro-layer). As shown in Fig. 3a, the performance curves of these three carbon cloth configurations follow the similar quantitative trend in the low and medium current density region; however

Table 3 – Macro- and micro-porous layer configurations of the tested cathode DM materials

Cathode		Configuration
Macro-DM substrate	Micro-porous layer	notation
Gore™ Carbel CL®	Case 1: None	Case 1: C
	Case 2: Gore™ CARBEL® MP30z	Case 2: C+M
	Case 3: Carbon/PTFE coating	Case 3: C+C
Sigracet™ SGL 10BA®	Case 1: None	Case 1: NW
	Case 2: Gore™ CARBEL® MP30z	Case 2: NW+M
	Case 3: Carbon/PTFE coating	Case 3: NW+C
Toray™ TGP 60®	Case 1: None	Case 1: P
	Case 2: Gore™ CARBEL® MP30z	Case 2: P+M

exhibit significant deviations at high current density region (>1200 mA/cm^2), in which the concentration polarization dominates. Similarly, the measured mass transfer resistance (R_{MT}) is observed to deviate in the high current density region (>1200 mA/cm^2), in agreement with the observed performance drop. Compared to the tested Carbel cloth DM combinations, the C+M configuration exhibits a dramatic increase in the mass transfer resistance at high current, indicating the highest tendency among the tested configurations to flood under wet conditions. On the other hand, the use of Carbel CL cloth coated with the carbon/PTFE coating (C+C configuration) has minimum mass transport resistance, therefore yielding the best performance within the same high current density region.

3.1.1.2. Non-woven Series. A similar type of comparison was also performed for three different configurations of the non-woven DM substrates. Fig. 3b represents the polarization curves of SGL 10BA non-woven (NW) DM namely, bare NW,

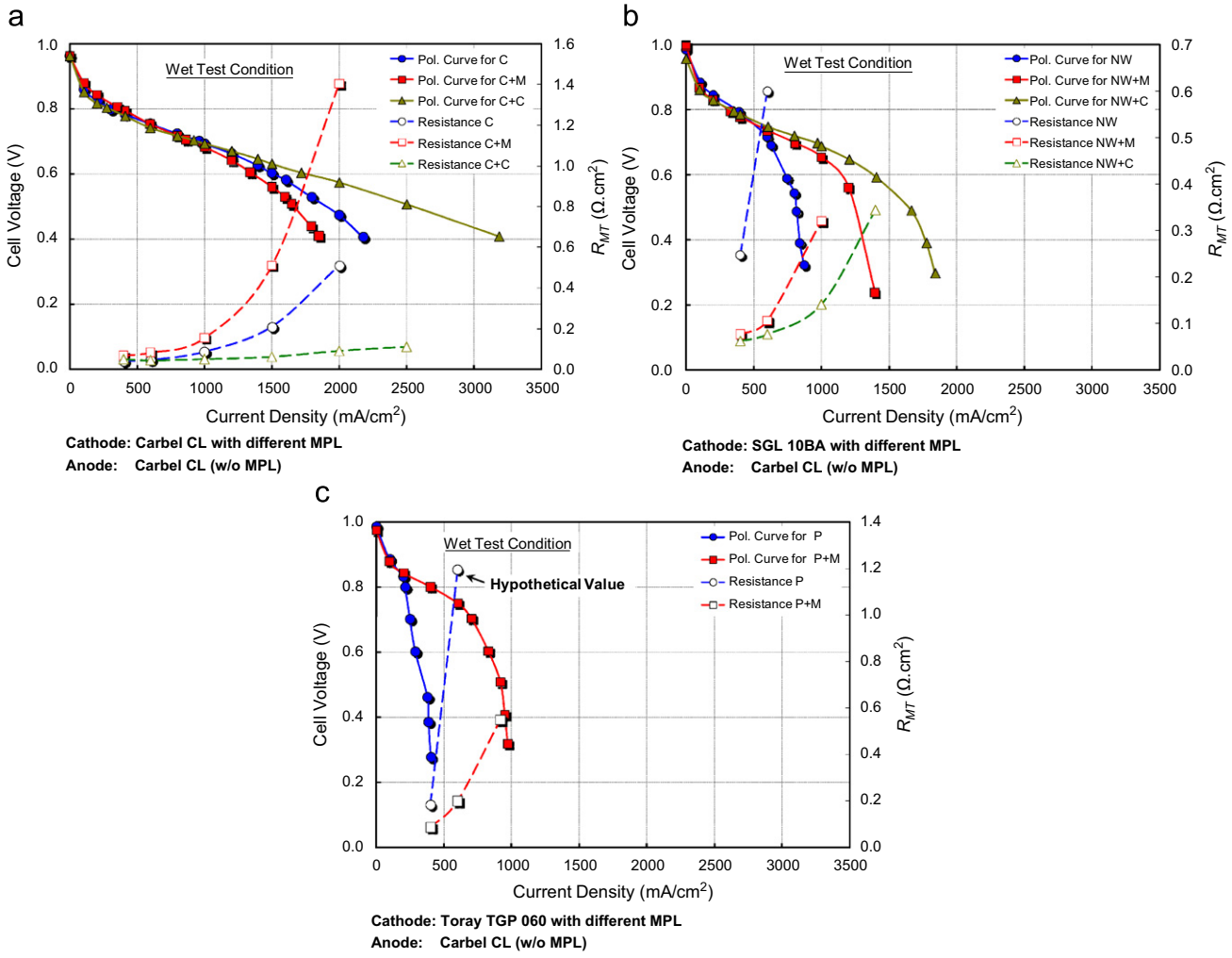

Fig. 3 – Performance and mass transfer resistance (R_{MT}) comparison of three basic types of DM materials with different MPL configurations on cathode electrode under wet conditions: (a) Carbel CL cloth (C); (b) SGL 10BA non-woven (NW) and (c) TGP 060 paper (P). (Note that Carbel CL cloth without MPL served as anode DM in all cases.)

NW+M (with MP30z micro-layer) and NW+C (with carbon/PTFE micro-layer). From the polarization curves and the measured mass transfer resistance values (Fig. 3b), the carbon/PTFE coated DM configuration (NW+C) is observed to yield the best performance in extremely wet conditions, whereas the bare non-woven DM (NW) exhibits a very high mass transfer resistance (~1200 mΩ cm^2 at 600 mA/cm^2), thus experiencing severe flooding even at low and moderate current density regions (i.e., <600 mA/cm^2).

3.1.1.3. *Paper series*. Fig. 3c shows the performance of two tested configurations of paper type (P) Toray 060 DM samples namely, bare P, and P+M (with MP30z micro-layer). As seen in Fig. 3c, addition of MP30z micro-layer to the base Toray paper substrate appears to reduce mass transfer resistance, thus improving the cell performance. However, both configurations of Toray paper DM samples exhibit relatively lower overall cell performance compared to the ones obtained with Carbel CL cloth and non-woven SGL 10BA DM samples due to severe flooding in the bare paper. The maximum operating current density for the bare Toray paper DM sample is only 400 mA/cm^2. Note that since the base Toray paper DM substrate cannot handle flooding-free operation even at low current, the mass transfer resistance data point shown at 600 mA/cm^2 in Fig. 3c denotes *the hypothetical value* projected from R_{MT} at 400 mA/cm^2 based on the slope of the measured polarization curve.

3.1.1.4. *Cross-comparison*. A cross-comparison of bare Carbel CL cloth (C), bare SGL non-woven (NW) and bare Toray paper DM (P) samples in combination with the different MPLs was performed. Fig. 4 represents the performance curves using the bare Carbel CL cloth, SGL non-woven and Toray paper DM substrates as a DM on the cathode electrode. The performance curves shown in Fig. 4 indicates that the use of bare Carbel CL cloth DM yields higher fuel cell performance than the bare non-woven and the paper families DM samples under the wet condition. This observation may indicate the higher water retention capacity of the Carbel CL cloth compared to the non-woven SGL and Toray carbon paper DM. This favorable characteristic of Carbel CL cloth might facilitate the removal of the generated water from the reaction sites.

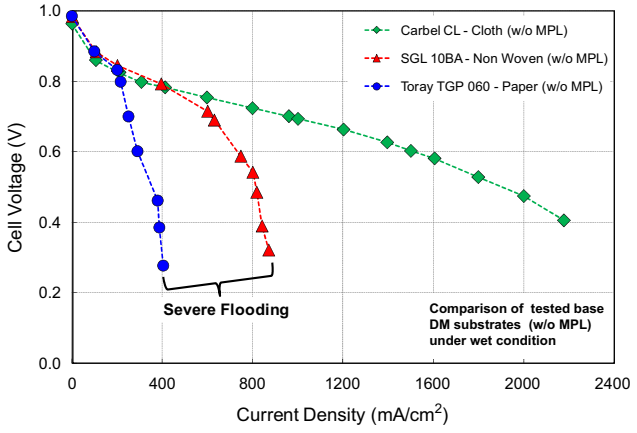

Fig. 4 – Performance comparison of bare cloth, non-woven and paper under wet condition.

The inclusion of carbon/PTFE coating to the base cloth (Fig. 3a) and non-woven DM samples (Fig. 3b) appears to improve the mass transport ability, yielding higher fuel cell performance under the wet condition than the bare cloth (C) and non-woven (NW) substrates. The improvement in cell performance stems from the inclusion of carbon/PTFE micro-layer, which acts a capillary barrier at the catalyst layer interface. The addition of MPL induces an additional liquid water resistance at the cathode CL–DM interface. The enhanced resistance directs the liquid flow to the anode through the membrane, thus reducing the water coverage of the cathode, and as discussed, also serves as a saturation discontinuity, keeping a high open pore volume for the reactant transport in the cathode catalyst layer.

In contrast to the positive impact of adding carbon/PTFE coating, the inclusion of MP30z to the bare DM samples tested manifests inconsistent effects on the cell performance. The addition of MP30z layer to bare non-woven (Fig. 3b) and paper DM (Fig. 3c) was observed to improve the mass transfer, and consequently cell performance; however it significantly reduces the cell performance when paired with cloth DM (Fig. 3a). This interesting finding suggests the existence of a complex interaction between the macro- and micro-layers, which cannot be explained through the capillary flow concept alone, since the PTFE content, pore size and porosity are approximately the same between these samples. Local morphological and thermal effects are likely responsible for this difference. But in general, at high water content levels (i.e. depending on the operating temperature and relative humidity), the inclusion of MPL plays a beneficial role of directing the liquid water toward the anode across the membrane by inducing a high capillary barrier (i.e. existence of minute pores at the interface), which indirectly improves the mass transfer performance (i.e. decreases the mass transfer resistance), and therefore reduces the flooding level on the cathode DM.

3.1.2. *Cathode performance under dry condition*

Under dry conditions, the polymer electrolyte membrane can experience severe dehydration that causes significant reduction in ionic conductivity of the membrane. The reduction in ionic conductivity of the membrane promotes the increase of the ohmic losses, reducing cell performance [44]. Therefore, in order to alleviate the negative effects of dry environments, the DM should be designed to retain water inside the MEA without causing mass transfer limitation for the reactant flow. In that manner, the choice of DM architecture is one of the key factors to achieve a lower membrane resistance (R_{MEA}) during the cell operation under dry conditions.

The performance curves and the corresponding membrane resistance of all three configurations of the base Carbel CL cloth DM under dry condition are shown in Fig. 5. It should be noted that the MEA resistance (R_{MEA}) herein represents the hydration state of the MEA, thus it is different than the ohmic resistance of the fuel cell. It was calculated based on the results of *in situ* and *ex situ* impedance experiments upon eliminating the ohmic resistances of other electrically

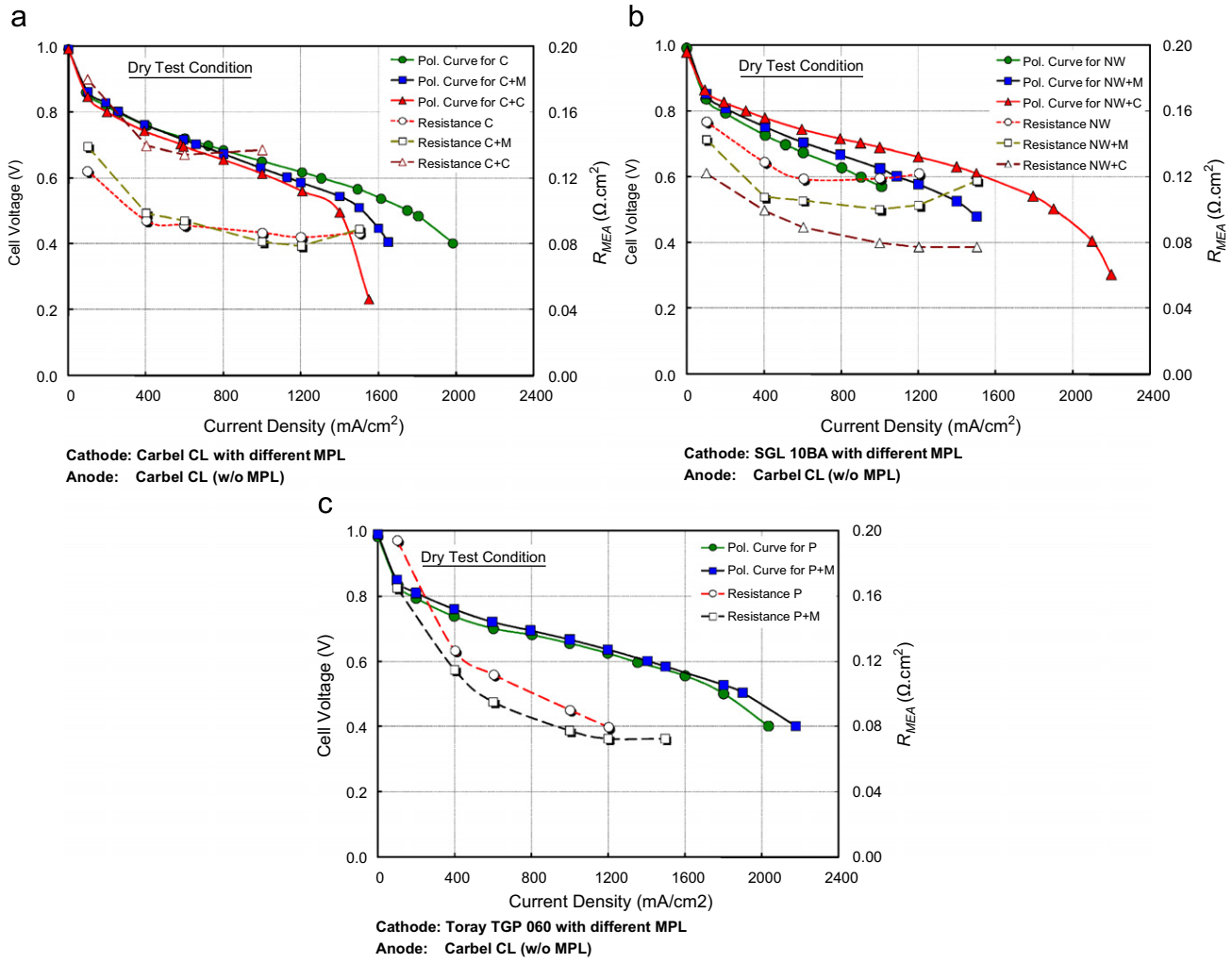

Fig. 5 – Performance and mass transfer resistance R_{MT} comparison of three basic types of DM materials with different MPL configurations on cathode electrode under dry conditions: (a) cloth (C); (b) non-woven (NW) and (c) paper (P). (Note that Carbel CL cloth without MPL served as anode DM in all cases.)

conducting components of the fuel cell. The detailed description regarding the measurement of MEA resistance, mass transfer resistance and other resistances is provided in Appendix A. Similar to the experiments under wet conditions, the bare Carbel CL substrate (without MPL) was used on the anode side in all three configurations.

3.1.2.1. Cloth series. When the performance of different cloth DM configurations are compared, the bare Carbel CL cloth without the inclusion of any micro-layers (Fig. 5a) is observed to yield the best cell performance under dry conditions. The results indicate that the use of bare Carbel CL cloth on the cathode provides the most hydrated environment for MEA under dry conditions. However, even though using the proper DM configuration can reduce the dehydration of MEA, it should be noted that the membrane is still exposed to an extremely dry environment; therefore the fuel cell experiences a lower performance than those under wet condition.

The other two configurations of the Carbel Cloth DM (i.e. one coated with carbon/PTFE layer and the other one with MP30z micro-layer) exhibit different behavior, however both yielded lower performance than that of bare Carbel cloth case (Fig. 5a). To further understand the origin of the difference in performance, the MEA resistances of these two configurations were measured by AC impedance. The AC impedance analysis revealed that R_{MEA} for C+M configuration was lower than that of C+C, suggesting that the inclusion of MP30z micro-layer assists in keeping the MEA more hydrated than the carbon/PTFE coating. This can be possibly attributed to relatively smaller pore size of the MP30z than that of the carbon/PTFE coating, which pushes more water toward anode through the membrane.

Physically, the pore size effect can be explained through the concept of pore entry pressure. At a microscopic level, transport of liquid droplets from one pore to another pore requires a pressure gradient, which must exceed the pore entry pressure. The pore entry pressure is defined as the pressure required for non-wetting phase to intrude into that pore, since wetting phase is preferentially adsorbed by the pore surface; therefore does not require any threshold pressure to occupy the pore. The pore entry pressure depends upon the dimension of the pore, hydrophobicity and surface

contact angle. Therefore, the porous medium having small pore size experiences higher resistance to the liquid flow due to the higher pore entry pressure. In that manner, in a hydrophobic pore space of DM, liquid water transport preferentially takes places in large pores due to the lower resistance; while gas phase flows through the small pores.

To further confirm this reasoning, additional experiments using the same cell hardware with no fuel and oxidant gases were performed to measure the bulk electronic resistance of the carbon/PTFE layer and MP30z micro-layer. A series of independent AC measurements revealed that the inclusion of MP30z micro-layer to the Carbel CL cloth resulted in about 7 mΩ cm^2 higher electronic resistance than the inclusion of carbon/PTFE coating. This additional finding suggests that using the C+M configuration exhibits the beneficial feature of providing a more hydrated environment for MEA; however this beneficial feature is suppressed to some extent by the negative effect of inducing a higher electronic resistance that causes a reduction in the overall cell performance.

3.1.2.2. Non-woven and paper series. For non-woven SGL 10BA DM series, the samples coated with the carbon/PTFE layer (NW+C) were observed to yield the best cell performance with the minimum MEA resistance among the other non-woven configurations, as shown in Fig. 5b. This can be attributed to the existence of carbon/PTFE micro-layer, which aids in keeping the membrane hydrated as it directs the generated water to the polymer membrane. The performance curves and R_{MEA} values of Toray 060 paper DM configurations (i.e. Toray 060 carbon paper DM with and without MP30z micro-layer) under dry conditions are also shown in Fig. 5c. Unlike non-woven and cloth types, the results for the Toray paper DMs indicate that the addition of a micro-layer (MP30z) did not significantly alter the performance of bare paper DM under dry conditions, while the addition of MP30z membrane layer to Toray 060 paper substrate under wet conditions is observed to greatly improve the cell performance. The apparent discrepancy in the cell performance upon the inclusion of MP30z micro-layer to Toray paper DM under wet and dry conditions also confirms the existence of a strong and complex interfacial interaction between the macro- and micro-layers.

3.1.3. Comparison of cathode DMs for versatile operation

Facing the increasing demand of delivering robust operations during automotive driving cycles where extremely different conditions are imposed, choosing the proper DM combinations on anode and cathode electrode is critical to achieve favorable micro-fluidic management in an operating fuel cell. For that purpose, additional resistance measurements were performed to analyze the sustainability of the tested cathode DM samples under versatile operations.

Fig. 6a shows the measured R_{MT} values under wet conditions versus the measured R_{MEA} values of the tested DM configurations used on the cathode under the dry condition. The mass transfer resistance measurements were performed at 1500 mA/cm^2, whereas the membrane resistance was measured at 400 mA/cm^2. While different DM configurations were tested in the cathode, a bare Carbel CL cloth DM substrate (without MPL) was used in the anode electrode for

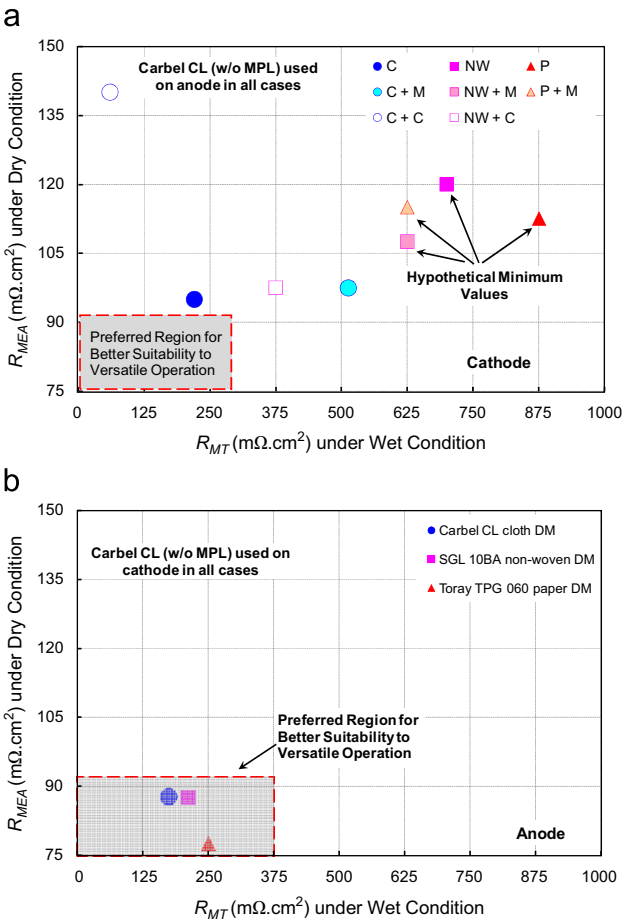

Fig. 6 – Comparison of performance of different DM–MPL combinations for versatile operation under two extreme conditions (wet and dry): (a) cathode and (b) anode. The hypothetical minimum data points indicate the value of its mass transfer resistances at maximum operable current density for that DM–MPL combination.

all these experiments. Note that the R_{MT} values of the bare and the MP30z coated non-woven SGL 10BA DM samples were plotted at their hypothetical minimum[1] values shown in Fig. 6a, since the high mass transfer resistances of these two DM configurations did not allow the cell to reach the specified current density of 1500 mA/cm^2 under wet condition. For robust and efficient cell operation, the DM should preferably achieve the lowest possible R_{MT} under wet conditions, and at the same time, it should provide favorable environment for MEA to yield the lowest possible R_{MEA} under dry conditions. Based on this concept, the region marked as 'preferred region of operation' on the lower left corner of Fig. 6a represents the target or the most favorable region, where both the R_{MT} and R_{MEA} values should preferably fall in for a versatile operation.

[1] The hypothetical minimum values for R_{MT} indicate the mass transfer resistances at the maximum operable current density and does not reflect the R_{MT} obtained at 1.5 A/cm^2 as for other cases.

Table 4 – Performance ranking of the anode DMs based on their values of mass transfer and MEA resistances under wet and dry conditions, respectively

Rank	Wet condition (based on least R_{MT})			Dry condition (based on least R_{MEA})		
	Cloth (Carbel®)	Non-woven (SGL 31®)	Paper (TGP 060®)	Cloth (Carbel®)	Non-woven (SGL 31®)	Paper (TGP 060®)
1	C+C (1)	NW+C (4)	P+M (6)	C (3)	NW+C (1)	P+M (2)
2	C (2)	NW+M (5)	P (8)	C+M (5)	NW+M (6)	P (4)
3	C+M (3)	N (7)		C+C (7)	NW (8)	

As shown in Fig. 6a, the measured data for the tested DM configuration on the cathode electrodes does not follow any particular trend, thus complicating the task to perform a proper judgment regarding the selection of most suitable or beneficial DM–MPL combination for wet and dry conditions. Table 4 presents the ranking of the tested DM samples (on the cathode) based on their suitability to a particular operating condition. The numbers inside the brackets denote the overall ranking of the DM among the eight different DM–MPL combinations under dry or wet conditions. Variation in the performance trend of the MPL selection with macro-DM can also be observed from the overall rank given in Table 4. For example, the Carbel CL cloth coated with carbon/PTFE micro-layer is observed to yield the best performance in the cloth family under wet condition, whereas the bare Carbel CL cloth performs best under dry condition. Moreover, the Toray 060 paper DM in general has much better performance under dry conditions, but is ranked as the worst under wet conditions.

The conflicting observation among the different DM configurations on the cathode also suggests that the capillary transport concept alone is not sufficient to accurately determine the most favorable macro-DM and MPL configuration that would be capable of removing the excess water out of the MEA under wet conditions, while retaining the water inside the MEA under dry conditions.

3.1.4. *Summary of DM–MPL interaction on the cathode*

The results presented in previous sections indicate that there is no apparent simple or distinct parameters (i.e. contact angle, pore size, porosity, etc.) that can accurately characterize the interactions between the macro- and micro-porous layers of a cathode electrode. While the current results reveal the existence of a strong interaction between micro- and macro-layers, the inclusion of MPL to the bare DM substrates is observed to yield dissimilar impact on the cell performance. For instance, addition of MP30z layer to the bare non-woven SGL DM sample (NW) and Toray 060 paper DM (P) is observed to increase the fuel cell performance under wet conditions. However, use of the same MP30z porous layer on Carbel Cloth DM is found to yield a lower cell performance under wet condition, indicating that the performance of MPL is not solely dependent on its intrinsic bulk properties, but also on the nature of its interfacial interactions with the macro-porous DM substrate.

This hypothesis is also confirmed by the measured magnitude of the variations in R_{MEA} and R_{MT} upon the inclusion of MP30z and carbon/PTFE micro-layers on bare cloth, non-woven and paper macro-porous DM samples. If the performance of fuel cell was dependent on the bulk property of MPL or DM alone, one would expect identical values for R_{MEA} or R_{MT} for a particular type of MPL, regardless of the type of macro-DM used. Therefore, based on these observation, it can be concluded that the interfacial effects cannot be described through concept of multi-phase transport alone (i.e. pore size and hydrophobicity). Therefore, an appropriate approach would consider the variations in local morphology, thermal conductivity and phase change, which have high impact on the interfacial effects.

3.2. *Effects of anode DM on cell performance*

While the continuous water generation in the cathode assists in providing a favorable hydrated environment for the MEA, the only source of water on the anode side is the moisture in the feed stream and the back-diffusion of water from the cathode. Similar to the conditions tested on the cathode side, different DM samples were tested on the anode side under dry and wet conditions to identify the impacts of the anode DM material on the cell performance.

In these experiments, three types of DM materials were tested as the anode, including: bare Carbel CL (C), bare SGL31BA (NW) and bare TGP 060 (P). While these three different base DM substrates were separately tested in the anode, the Carbel CL cloth was used as the cathode DM in all three cases. The cell performance for these three types of DM materials was analyzed under both wet and dry conditions. Fig. 6b shows the measured R_{MT} values measured under the wet conditions versus the measured R_{MEA} values under dry condition of these three types of anode DM samples. As seen in Fig. 6b, the measured R_{MT} and R_{MEA} values of all three DM materials tested on anode electrode are observed to fall into the preferred region, providing the desired performance under these extreme conditions (wet and dry conditions). In other words, there is no noticeable difference in the cell performance due to the change in anode DM material, and the type of DM used in the anode does not appear to have a strong impact.

3.3. *DM wettability and fuel cell performance*

The degree of PTFE loading in DM plays a deterministic role in the multi-phase transport mechanism, since any increase in

Table 5 – Four different operating conditions used for the investigation of PTFE effect on cell performance

Condition	Automotive wet	Stationary	Encore	Automotive dry
Temperature, °C	60	70	80	95
Inlet RH (H_2/air), %	100/100	100/100	75/0	50/0
Outlet RH[a] (Air), %	305	160	120	69

[a] Calculated based on a mass balance of water in fuel cell cathode at 1 A/cm^2, and 100% inlet relative humidity, assuming no crossover.

PTFE loading facilities the water removal rate from the hydrophobic pores, therefore leading to a considerable reduction in the water retention (water storage in a hydrophilic pore) capacity of the DM [35]. However, the engineering consequences of increasing PTFE content in the DM should be systematically optimized in order to minimize the additional losses introduced by addition of this hydrophobic agent. The negative influences may manifest as: (i) a decrease in porosity and oxygen diffusion [45], and (ii) an unfavorable increase in the electric resistance of the DM [46].

In order to examine the impacts of PTFE content on the cell performance, additional tests were performed for differently engineered base DM materials including Carbel CL cloth and non-woven SGL 10 series. The effects of addition of hydrophobic agent (PTFE) into the bare anode and cathode DM (both without MPL) on the fuel cell performance was evaluated under four different operating conditions, namely, automotive wet, stationary, encore and automotive dry. The detailed descriptions of these testing conditions are given in Table 5. The testing conditions were designed in such a way to cover all extreme conditions that a fuel cell can be exposed to. Among these four conditions, the automotive wet condition possesses the highest tendency to flood due to its highest average outlet RH (305%),[2] whereas the automotive dry condition yields the lowest tendency to promote flooding, as given in Table 5.

Fig. 7 shows the performance curves of the bare cloth and non-woven DM samples with and without 5% PTFE treatment under four different operating conditions. The performance curves experience some variations with the addition of PTFE agent in the low current region (ranging from 250 to 500 mA/cm^2) under automotive wet condition (Fig. 7a). This can be attributed to the fact that the effect of PTFE coating on the cell performance is a strong function of the water removal rate, which is directly linked to the nature of the operating environment. At low current, the DM is exposed to less water generation. Therefore, the effect of PTFE on cell performance is less pronounced.

At higher current densities ($>$500 mA/cm^2), the addition of PTFE has a strong impact on the performance. As the DM is exposed to more liquid water at high current density, the wettability characteristic of the DM becomes more dominant on the cell performance. Accordingly, the addition of PTFE has improved the cell performance considerably under automotive wet conditions in high current density region (Fig. 7a), whereas it slightly enhances the performance under stationary conditions in the same current density region (Fig. 7b). The cell operating under automotive wet conditions is prone to be exposed more liquid water, and an increase in the hydrophobic characteristic of pore structure promotes the removal of excess liquid water, improving the cell performance. Therefore, effect of addition of hydrophobic agent to the DM substrates is more pronounced under wet conditions. In terms of operations in encore and automotive dry conditions, no noticeable change in performance is observed with addition of PTFE under the encore (Fig. 7c) and automotive dry (Fig. 7d) conditions, possibly due to relatively drier environment.

In summary, addition of PTFE to macro-DM improves the cell performance under wet conditions; therefore such a hydrophobic treatment is essential to alleviate the flooding effect under wet conditions. However, as the operating condition becomes drier, this beneficial effect of hydrophobic coating gradually diminishes.

3.3.1. *Capillary transport mechanism*

Physically, the observed effects of PTFE content on the cell performance under dry and wet conditions can be linked to the alteration in capillary transport mode. The liquid water transport within the pores of the DM is mainly governed by capillary action. In the capillary transport mode, the driving force is created by the local capillary pressure gradient, which shows a strong dependence on the water saturation and the wettability of the pore matrix [33].

Recently, our group has performed an extensive study focused on benchmarking the capillary transport characteristics of differently engineered DMs [34]. The drainage capillary pressure-saturation curves of the hydrophobic pores for the SGL 24 series DM samples coated with different PTFE loadings (5%, 10% and 20% by wt) were measured via the method of standard porosimetry to quantify the corresponding change in capillary pressure as a function of PTFE loading of the DM.

Fig. 8 shows the measured characteristics capillary pressure-saturation curves for the SGL 24 series DM samples treated with different PTFE loadings, namely: SGL 24BC (5% PTFE by wt), SGL 24CC (10% PTFE by wt) and SGL 24DC (20% PTFE by wt). As shown in Fig. 8a, the individual capillary pressure-saturation curves follow similar trends. However due to the different PTFE contents, the measured capillary pressure values differ over the entire liquid saturation spectrum. The highest capillary pressure is observed in SGL

[2] Calculated based on a mass balance of water in fuel cell cathode at 1 A/cm^2, and 100% inlet relative humidity, assuming no crossover.

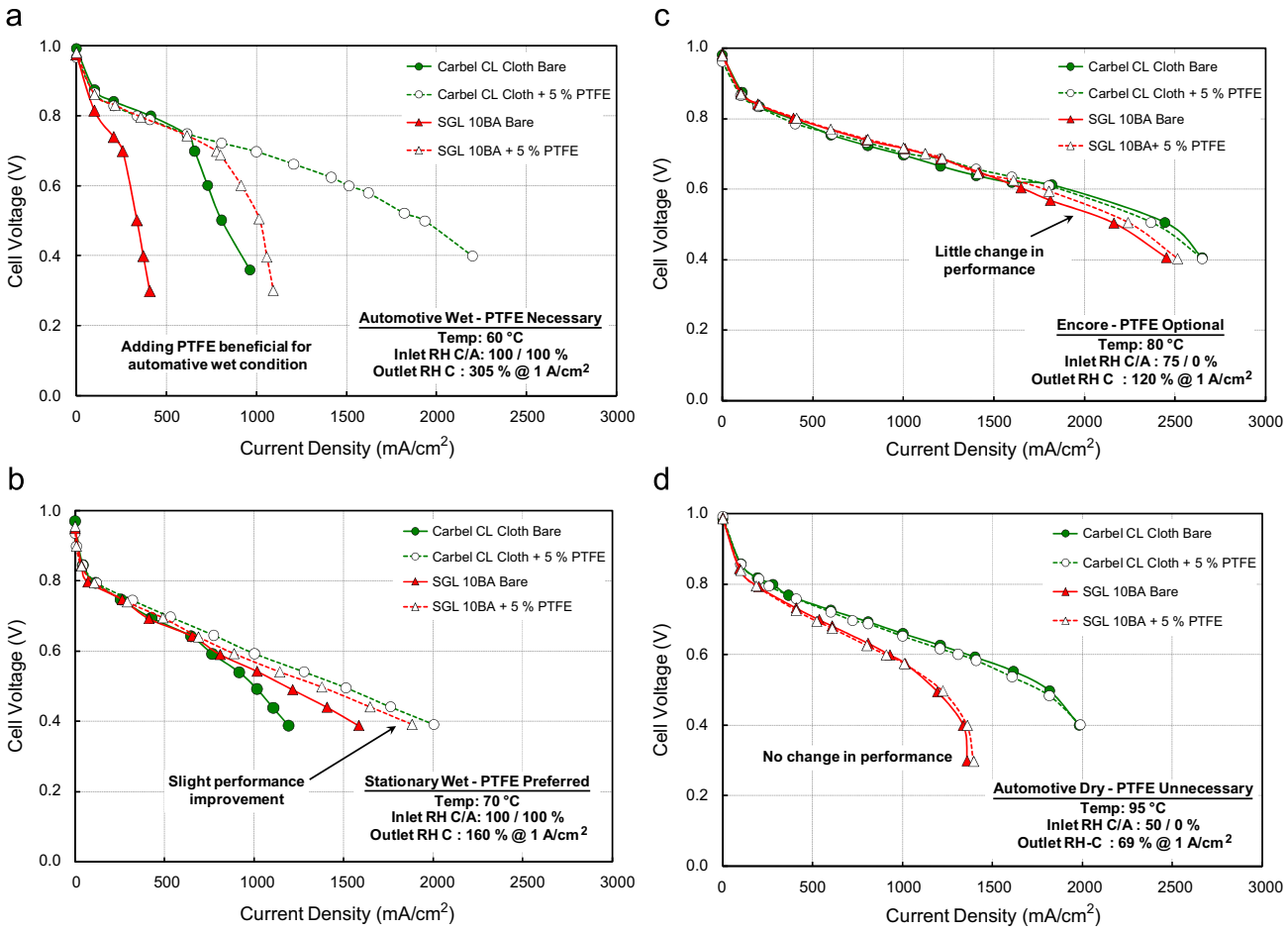

Fig. 7 – Performance curves of bare (without MPL) cloth and non-woven DM with and without 5% PTFE treatment under four different operating conditions: (a) automotive wet; (b) stationary; (c) encore; and (d) automotive dry.

24DC treated with 20% PTFE, whereas the lowest value at a given saturation is observed in SGL 24BC treated with 5% PTFE. This behavior can be attributed to the strong dependence of capillary pressure on the hydrophobicity of the pore matrix. Physically, at pore level, rendering the carbon fiber more hydrophobic distorts the molecular force balance at the interface, forcing the liquid water to move toward an unstable state. The enhanced imbalance at the phase interface promotes a higher capillary pressure inside the pore, therefore facilitating the water removal from the pore matrix of the DM.

In addition, the water retention capacities of these three SGL 24 series DM samples were measured via spontaneous capillary imbibition tests. Note that the spontaneous capillary imbibition is a natural process and requires existence of interconnected hydrophilic pores. For more information about these experiments, one can refer to. The results show that uncompressed SGL 24BC treated with 5% PTFE content imbibes a maximum of 0.35 saturation; whereas uncompressed SGL 24DC tailored with 20% PTFE can only imbibe a maximum of 0.28 saturation [34]. Physically, this can be attributed to the fact that rendering the DM more hydrophobic decreases the total connected hydrophilic pathways, thus reducing the potential water retention or storage capacity.

3.4. *Effects of long-term fuel cell operation on DM morphology*

Prolonged fuel cell operations may expose the DM to unfavorable environments, accelerating the internal structure degradation of the DM. In terms of DM properties, the wettability and the water retention capacity are two governing parameters that significantly influence the performance. While the hydrophobicity (wettability) of the DM enables effective drainage of liquid water from the active electrochemical sites, the water retention characteristic governs the tendency of the DM to imbibe and store liquid water within the pore matrix. In addition, during the prolonged fuel cell operation, the DM may experience various compression loadings and thermal cycles. This generate strong local stresses that can alter the morphological structure, consequently the multi-phase transport characteristics of the fuel cell DM. Additional experiments were performed to diagnose the changes in the governing transport properties of the tested DM samples under long-term operations.

3.4.1. *Water retention capacity (water uptake ratio)*

The water retention capacity (water storage) is a characteristic property of a fuel cell porous DM, and it represents the available connected hydrophilic pore space of a fuel cell DM

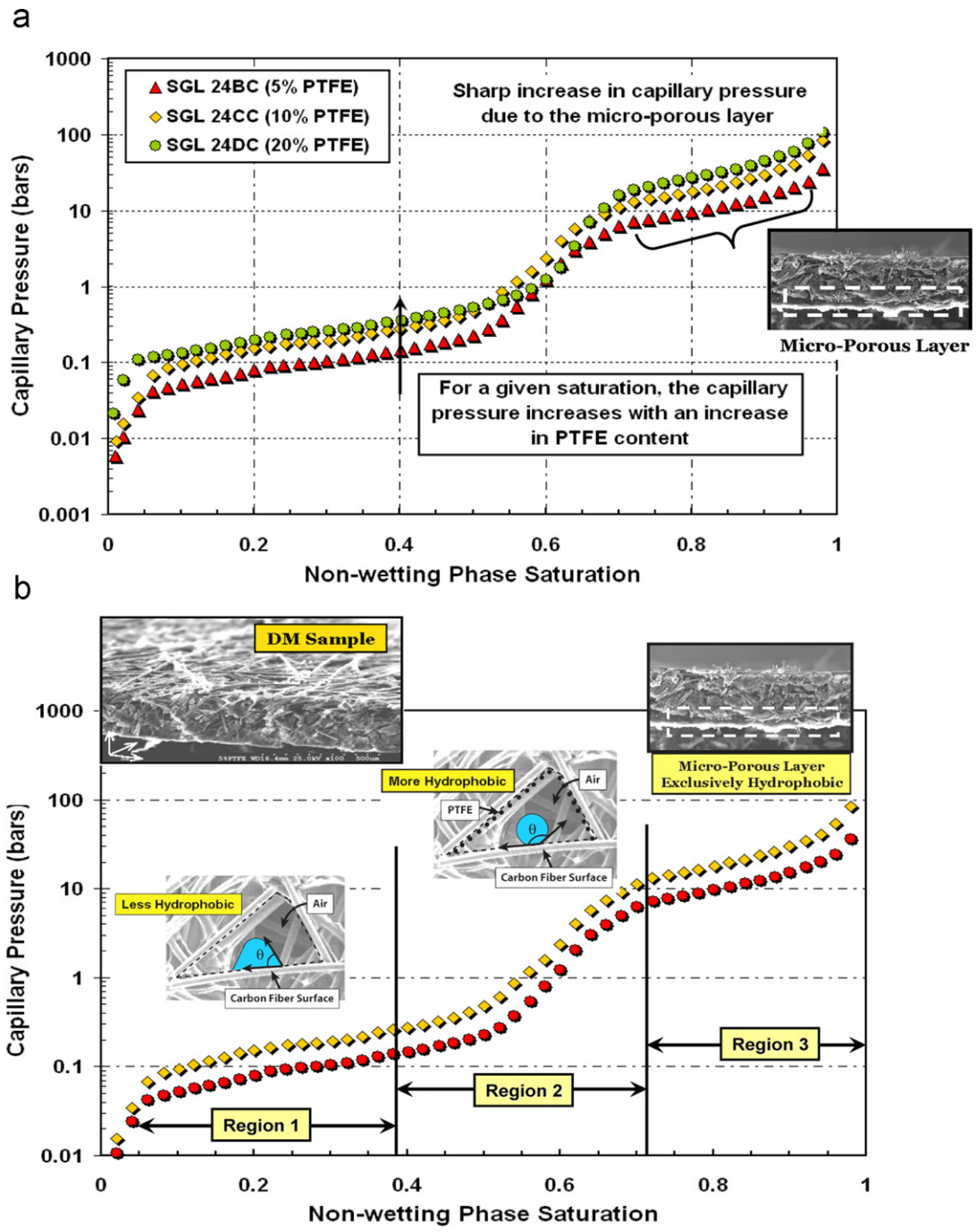

Fig. 8 – (a) Measured capillary pressure versus non-wetting phase saturation of SGL 24 series non-woven DMs coated with different PTFE loadings at room temperature under no compression, and (b) schematic of three distinct regions observed in the measured capillary pressure-saturation curves of tested DM samples.

that can be spontaneously imbibed and occupied by liquid water. The liquid water content stored (water retention capacity) in the DM during operation is critical for freeze/thaw, start-up, degradation, stability and purging [47,48] operations.

Ex situ experiments were performed for two different DM samples, namely non-woven SGL 10BA (without MPL) and SGL 10BB coated with MPL. The SGL 10 series DM samples were chosen for this specific test, since they are widely used in long-term fuel cell operations. The tested SGL 10 series DM samples are coated with 5% PTFE and have a thickness of 400 μm. In these experiments, both virgin and aged (used for a certain period of time in a fuel cell operation under wet condition specified in Table 2) DM samples were soaked in water at 80 °C for several days, and the weight of these tested DM samples were measured at frequent intervals to determine the amount of water absorbed by the DM.

Fig. 9 shows the amount of water uptake ratio or water retention capacity of the virgin and aged DM samples

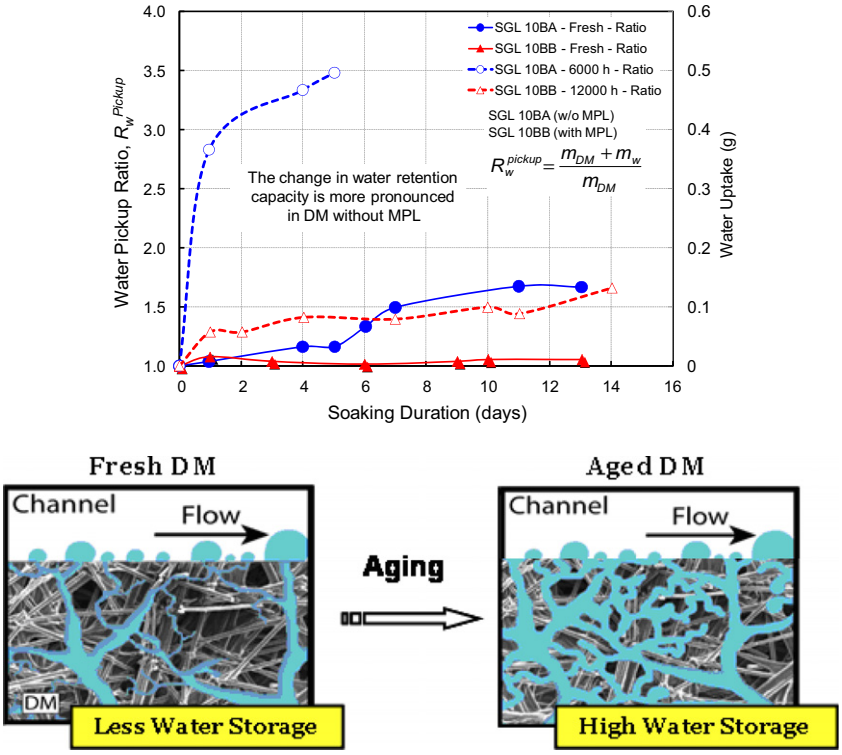

Fig. 9 – The effect of long-term fuel cell operation on the performance, i.e. the amount of water picked up over time at 80 °C by both fresh and aged SGL 10 series DM samples (with and without MPL) under soaked conditions.

(i.e. used in actual fuel cell operation for 6000 and 12 000 h) as a function of soaking duration. The water uptake ratio (R_w^{pickup}) represents the weight ratio of the soaked to un-soaked DM samples and given by

$$R_w^{pickup} = \frac{m_{DM} + m_w}{m_{DM}} \quad (1)$$

where m_{DM} and m_w represent the weight of dry DM and absorbed liquid water, respectively. Note that despite the existence of hydrophobic agent coating, the liquid water can still be absorbed into the DM through the fraction of surface pores that are hydrophilic in nature.

The results shown in Fig. 9 reveal that regardless of the type of DM materials, the virgin DM samples appear to absorb the liquid water at a much slower rate than that of aged DM samples. This can be attributed to the possible loss of hydrophobicity in the aged DM samples because of the prolonged fuel cell operations, in good agreement with the findings presented by Borup et al. [49]. In a study by Borup et al., the aged DM samples are observed to experience loss of hydrophobicity. Furthermore, the fiber contact angle measurements also confirm the significant decrease in the internal contact angles of the aged DM samples (even below 90°). These previous findings indicate the existence of a possible transition to a more hydrophilic state during long duration operation. Physically, the DM undergoing prolonged fuel cell operations is exposed to a direct contact with the water for a considerable period of time. During this period, the condensed liquid water, which accumulates through the available pores of the DM, may cause a substantial change in the structure of carbon fibers, binder orientation or PTFE amount in the DM. The PTFE particles bonded to the solid pore matrix may be swept away by the accumulation of excess liquid water, which is followed by a significant loss in hydrophobicity of the DM, since any loss of hydrophobicity is closely related to the amount of PTFE particles bonded on the carbon fibers.

When the water retention characteristics of virgin and aged DM samples are compared for each DM type (SGL 10BA or SGL 10BB), the DM aging effect is observed to be more pronounced for the SGL 10BA case, whereas the SGL 10BB DM sample (coated with MPL) is least affected by the prolonged fuel cell operation even after 12 000 h, as shown in Fig. 9. In addition, the rate of water absorption for aged SGL 10BB samples is found to be much less than that of fresh SGL 10BA. While both virgin and aged SGL 10BB DM samples were able to retain most of their hydrophobic pores even after prolonged operation inside a fuel cell, the SGL 10BA DM sample suffered a considerable loss in hydrophobicity within 6000 h of fuel cell operation. The mass of water uptake into SGL 10BA and SGL 10BB samples were also shown in Fig. 9. Though the dry weight of these samples differ due to the presence of an MPL in SGL 10BB and lack of the same in SGL 10BA, the mass of water uptake follows the same trend as that of the water pickup ratio.

The difference in the observed degradation of the wettability characteristics of the tested SGL 10BB (with MPL) and the bare SGL 10BA samples can be attributed to the presence of a hydrophobic MPL. As previously mentioned, the MPL in general has a compact (small pores) and rigid structure, providing a higher hydrophobic resistance, which increases the required threshold capillary pressure to overcome the

surface energy of the minute pores of the MPL for spontaneous imbibition. Even when the nature of the capillary pressure-saturation curve of a bi-layered fuel cell DM (with MPL) is analyzed [33], the capillary pressure-saturation curve exhibits a continuous 'S' shape (shown in Fig. 8b), indicating the highly nonlinear relationship between the capillary pressure and the saturation. As shown in Fig. 8b, there is a sudden jump in the measured capillary pressure at high saturation region, possibly due to the sudden change in the pore size at the DM–MPL interface. The sudden vast increase in the measured capillary pressure also underlines the dominating effect of the interfacial resistance at the DM–MPL interface. As a result, the compactness and rigidity of MPL further hampers the imbibition of generated water through the minute pores of MPL substrate, therefore limiting the surface area of the MPL exposed to liquid water. This limited access of MPL impedes the loss of hydrophobicity, thus enabling to retain its hydrophobic characteristics compared to macro-DM substrate.

3.4.2. *Degradation of macro-porous DM substrate*

The results presented in the previous section suggest that the long-term degradation of DM occurs mainly due to the alteration of the governing transport properties in macro-porous DM substrate, not in the MPL. In order to further confirm this finding, additional AC impedance measurements were performed for aged and virgin DM samples, which were all coated with an MPL. The measurements were performed at a constant current density of 1 A/cm^2 in order to capture the possible changes in the wettability characteristics of the macro-DM substrate due to the flooding. In these experiments, SGL 10BA non-woven substrate coated with MP30z layer was used as a DM. In each experiment, the macro-DM substrate (bare SGL 10BA without MPL) was changed with a new bare SGL 10BA substrate and bare Carbel CL cloth DM substrate, while the MP30z MPL was never replaced (i.e. the same MP30z material were used in all these experiments).

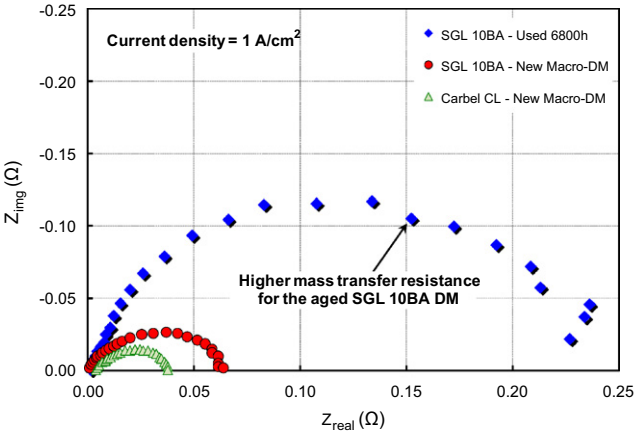

Fig. 10 – Nyquist plots of SGL 10BA with MP30z DM obtained after 6800 h fuel cell operation inside a fuel cell. Nyquist plots are also shown for the cases when the used macro-SGL 10BA was replaced by new macro-SGL 10BA and Carbel CL® DM samples on both anode and cathode sides.

The Nyquist plots shown in Fig. 10 represents the AC impedance measurements of aged SGL 10BA (i.e. used in a 6800 h operated fuel cell), virgin SGL 10BA and virgin Carbel CL cloth DM samples. It is worthwhile to re-emphasize that all the tested DMs were used with the same MP30z micro-layer. Therefore, keeping the same MPL layer in these composite DM samples enabled isolation of the changes in mass transfer resistance of the aged and virgin macro-DM substrates. As seen in Fig. 10, using virgin macro-DM substrate yielded a considerable decrease in the mass transfer resistance of the cell (approximately 75%) compared to the aged macro-DM substrate. However, the use of aged SGL 10BA macro-DM substrate (used in 6800 h operated fuel cell) caused the fuel cell to experience a significant mass transfer resistance possibly due to the degradation in wettability characteristics (i.e. loss of hydrophobicity), supporting the findings in the previous section. This observation also confirms the hypothesis that significant performance loss of the fuel cell during long-term operation is possibly dominated by the changes in the wetting properties of macro-porous DM substrate, not the micro-porous layer.

4. Conclusions

In this study, a detailed experimental investigation of macro- and micro-porous layer interaction in diffusion electrodes of PEFC was performed. Carbel Cloth, Toray 060 TPG 060 carbon paper, and SGL 10 and 31 series non-woven paper DM samples, in combination with carbon/PTFE coating and MP30z micro-layer have been subjected to extensive testing to delineate the role of macro-DM substrate and MPL on the short- and long-term fuel cell performance.

The results show that the type of DM used without MPL in the anode does not appear to have a strong impact on the cell performance under wet or dry condition, meaning that the selection of the macro-DM on the anode is not critical. The effects of cathode MPL were observed to exhibit different behaviors when applied to different macro-DM substrates, indicating that the existence of a complex interaction between the micro- and macro-layers of the porous diffusion electrodes that cannot be explained simply through the concept of capillary transport. Instead, a more complete understanding would be to account for the multi-phase transport characteristics with the interfacial heat transfer and phase change effects together. Furthermore, the present results reveal that the PTFE content in the macro-porous DM is found to have a dominant effect on the fuel cell performance during high humidity operation, but appears to have much less impact under dry conditions. Under long-term operation, the DM samples are observed to lose their hydrophobicity. Interestingly, the presence of an MPL mitigates the loss of hydrophobicity in the macro-porous DM, possibly due to the enhanced liquid resistance induced by the inclusion of MPL.

Finally, the present observations show that the interaction between the membrane and the DM is determined to be considerably different on both anode and cathode porous electrodes, indicating that the half cell multi-phase modeling approach considering only a single electrode would not be

appropriate. Therefore, for a more complete approach, the interfacial effects, heat transfer and phase change for both electrodes need to be characterized separately.

Acknowledgment

The authors are grateful to W. L. Gore & Associates Inc. for the assistance provided for this study. M. Mench wishes to thank NSF Career award for funding Dr. Kumbur in this work.

Appendix A. Methodology for analysis of EIS data

A.1. *In situ impedance measurement*

It is widely accepted that, when an AC impedance measurement is performed on an operating fuel cell, DM in the assembly can significantly impact the impedance in both high and low frequency ranges [50]. Based on this foundation, resistances at high and low frequency ranges were given special attention as they provided effective insights into the capability of DM to manage water.

For all the *in situ* AC impedance measurements, data were fitted with an equivalent circuit model (demonstrated in Fig. 2a) in order to extract resistances at different frequency ranges in a systematic manner. In this circuit model, *L* captures the effects of inductance, which can mostly be influenced by inductance behaviors of electronically conductive components of the whole measurement system. R_{HF} represents the HFR which is the sum of average resistance of the MEA (R_{MEA}) and electronic resistances from components such as DM (R_{DM}), cell hardware, wiring and connection (R_{other}). CPE1 and CPE2 are constant phase elements, which describe the distributed non-ideal capacitance of porous electrodes in the kinetic and mass transfer region. The response at medium frequency is described by R_k, which is assigned mostly to the electrode kinetic resistance for the oxygen reduction reactions. Finally R_{MT} describes response at low frequency, which reflects mass transfer resistance imposed by DM in a fuel cell system. The Nyquist plots obtained under wet and dry conditions were fitted to the circuit model described in Fig. 2a. Within the whole frequency range, the curve generated by the circuit model fits the experimental Nyquist data very well. Therefore, resistance values extracted from the circuit model, specifically, high frequency resistance R_{HF} and mass transfer resistance R_{MT}, can be used to assess the influence of DM on fuel cell performance.

A.2. *Ex situ impedance measurement*

The goal of performing the *ex situ* AC impedance measurements is to measure the resistance of the MEA at 60 °C and saturated condition. The accuracy of this value becomes crucial in the estimation of *in situ* MEA resistance in the extreme dry condition. As mentioned in the experimental section, *ex situ* AC impedance measurements were recorded in an inert (N_2) atmosphere to exclude possible electrochemical reactions. The spectra obtained under these conditions have features similar to those discussed in several publications by Pickup and coworkers [51,52]. A simple equivalent circuit model as shown in Fig. 2b, consisting of an inductor (L1), a resistor (R1) and a transmission line circuit (DX1) [51] was used to model the impedance response at each RH step. R1 represents the resistive component of the AC impedance of the MEA at each RH condition which is plotted as a function of RH, fitted by a power regression. The extrapolated 100% RH resistance value was used as the MEA resistance at 60 °C, which is represented as $R^{100\%}_{ex\ situ}$. For the MEAs tested in this study, the average value of $R^{100\%}_{ex\ situ}$ at 60 °C was measured to be 26 $m\Omega\,cm^2$.

A.3. *Estimation of R_{MEA} from in situ and ex situ measurements*

Although high frequency resistance R_{HF} can reflect hydration of the MEA, it consists of other components such as electronic resistance of DM, cell hardware, wiring and connections.

$$R_{HF} = R_{MEA} + R_{GDM} + R_{other} \tag{A.1}$$

In order to determine the influence of the DM on hydration of the MEA accurately, it is necessary to isolate R_{MEA} from the other components of R_{HF}. This was achieved by combining the information gathered through *in situ* and *ex situ* measurements. As mentioned in the experimental section, *in situ* measurements were carried out in two extreme conditions: the dry condition and the wet condition. The HFR in each case, R^{dry}_{HF} or R^{wet}_{HF}, was extracted from *in situ* AC impedance analysis. Based on Eq. (A.1), the following relationships were established:

$$R^{dry}_{HF} = R^{dry}_{MEA} + R^{dry}_{GDM} + R^{dry}_{other} \tag{A.2}$$

$$R^{wet}_{HF} = R^{wet}_{MEA} + R^{wet}_{GDM} + R^{wet}_{other} \tag{A.3}$$

R_{DM} or R_{other} does not depend on RH or temperature and therefore:

$$R^{dry}_{GDM} + R^{dry}_{other} = R^{wet}_{GDM} + R^{wet}_{other} \tag{A.4}$$

Meanwhile, R^{wet}_{MEA} must be equal to $R^{100\%}_{ex\ situ}$ obtained in the saturated *ex situ* measurement:

$$R^{wet}_{MEA} = R^{100\%RH}_{ex\ situ} \tag{A.5}$$

Combining Eqs. (A.2) through (A.5), one can calculate the average resistance of the MEA at the dry condition, R^{dry}_{MEA}, using the following relation:

$$R^{dry}_{MEA} = R^{dry}_{HF} - R^{wet}_{HF} + R^{100\%RH}_{ex\ situ} \tag{A.6}$$

In summary, two very important fuel cell performance parameters of DM were quantified using the methodology described above, namely; (a) R_{MEA} obtained from the combination of *in situ* and *ex situ* AC impedance analysis, and (b) R_{MT}, obtained from *in situ* AC impedance measurement. Since two extreme conditions were used to study the effects of DM, a total of four parameters R^{wet}_{MEA}, R^{dry}_{MEA}, R^{wet}_{MT} and R^{dry}_{MT} were obtained for each kind of DM evaluated.

REFERENCES

[1] Williams MV, Begg E, Bonville L, Kunz HR, Fenton JM. Characterization of gas diffusion layers for PEMFC. J Electrochem Soc 2004;151:1173.
[2] Chen-Yang YW, Hung TF, Huang J, Yang FL. Novel single-layer gas diffusion layer based on PTFE/carbon composite for proton exchange membrane fuel cell. J Power Sources 2007;173:183.
[3] Zhang F-Y, Suresh G, Advani SG, Prasad AK. Performance of a metallic gas diffusion layer for PEM fuel cells. J Power Sources 2008;176:293.
[4] Jiao K, Zhou B. Innovative gas diffusion layers and their water removal characteristics in PEM fuel cell cathode. J Power Sources 2007;169:296.
[5] Ge J, Higier A, Liu H. Effect of gas diffusion layer compression on PEM fuel cell performance. J Power Sources 2006;159:922.
[6] Han M, Chan SH, Jiang SP. Development of carbon-filled gas diffusion layer for polymer electrolyte fuel cells. J Power Sources 2006;159:1005.
[7] Jang J-H, Yan W-M, Shih C-C. Effects of the gas diffusion layer parameters on cell performance of PEM fuel cells. J Power Sources 2006;161:323.
[8] Escribano S, Blachot J-F, Etheve J, Morin A, Mosdale R. Characterization of PEMFCs gas diffusion layers properties. J Power Sources 2006;156:8.
[9] Prasanna M, Ha HY, Cho EA, Hong SA, Oh IH. Influence of cathode diffusion media on the performance of the PEMFCs. J Power Sources 2004;131:147.
[10] Kraytsberg A, Ein-Eli Y. PEMFC with improved water management. J Power Sources 2006;160:194.
[11] Pasogullari U, Wang CY, Chen KS. Two phase transport in polymer electrolyte fuel cells with bi-layer cathode gas diffusion media. J Electrochem Soc 2005;152:A1574.
[12] Wang CY. Fundamental models for fuel cell engineering. Chemical Reviews 2004;104:4727.
[13] Pasogullari U, Wang CY. Two phase transport and the role of microporous layer in polymer electrolyte fuel cells. Electrochim Acta 2004;49:4359.
[14] Vynnycky M. On the modelling of two-phase flow in the cathode gas diffusion layer of a polymer electrolyte fuel cell. Appl Math Comput 2007;189:1560.
[15] Koido T, Furusawa T, Moriyama K. An approach to modeling two-phase transport in the gas diffusion layer of a polymer electrolyte fuel cell. J Power Sources 2008;175:127.
[16] Xia ZT, Chan SH. Analysis of carbon-filled gas diffusion layer for H_2/air polymer electrolyte fuel cell with an improved empirical voltage–current model. Int J Hydrogen Energy 2007;32:878.
[17] He G, Zhao Z, Ming P, Abuliti A, Yin C. A fractal model for predicting permeability and liquid water relative permeability in the gas diffusion layer (GDL) of PEMFCs. J Power Sources 2007;163:846.
[18] Sui PC, Djilali N. Analysis of coupled electron and mass transport in the gas diffusion layer of a PEM fuel cell. J Power Sources 2006;161:294.
[19] Chang M-H, Chen F, Teng H-S. Effects of two-phase transport in the cathode gas diffusion layer on the performance of a PEMFC. J Power Sources 2006;160:268.
[20] Shi Y, Xiao J, Pan M, Yuan R. A fractal permeability model for the gas diffusion layer of PEMFCs. J Power Sources 2006;160:277.
[21] Song D, Wang Q, Liu Z-S, Huang C. Transient analysis for the cathode gas diffusion layer of PEM fuel cells. J Power Sources 2006;159:928.
[22] Inoue G, Matsukuma Y, Minemoto M. Evaluation of the thickness of membrane and gas diffusion layer with simplified two-dimensional reaction and flow analysis of polymer electrolyte fuel cells. J Power Sources 2006;154:8.
[23] Bultel Y, Wiezell K, Jaouen F, Ozil P, Lindbergh G. Investigation of mass transport in gas diffusion layer at the air cathode of a PEMFC. Electrochim Acta 2005;51:474.
[24] Nam JH, Kaviany M. Effective diffusivity and water saturation distribution in single and two layer PEMFC diffusion medium. Int J Heat Mass Transfer 2003;46:4595.
[25] Pisani L, Murgia G, Valentini M, D'Aguanno B. A working model of polymer electrolyte fuel cells. J Electrochem Soc 2002;149:A898.
[26] Van Nguyen T, Knobbe MW. A liquid water management strategy for PEM fuel cell stacks. J Power Sources 2003; 114:70.
[27] Djilali N. Computational modeling of polymer electrolyte membrane (PEM) fuel cells: challenges and opportunities. Energy 2007;32:269.
[28] Lin WH, Van Nguyen T. Modeling liquid water effects in the gas diffusion and catalyst layers of the cathode of a PEM fuel cell. J Electrochem Soc 2004;151:A1999.
[29] Weber AZ, Newman J. Modeling transport in polymer electrolyte fuel cells. Chem Rev 2004;104:4679.
[30] Gostick JT, Ioannidis MA, Fowler MW, Pritzker MD. Pore network modeling of fibrous gas diffusion layers for polymer electrolyte membrane fuel cells. J Power Sources 2007;173:277.
[31] Turhan A, Heller K, Brenizer JS, Mench MM. Quantification of liquid water accumulation and distribution of in a polymer electrolyte fuel cell using neutron imaging. J Power Sources 2006;160:1195.
[32] Dong Q, Kull J, Mench MM. Real time water distribution in a polymer electrolyte fuel cell. J Power Sources 2005;139:106.
[33] Kumbur EC, Sharp KV, Mench MM. Liquid water droplet behavior and instability in a polymer electrolyte fuel cell flow channel. J Power Sources 2006;161:333.
[34] Kumbur EC, Sharp KV, Mench MM. Validated leveret approach for multiphase flow in PEFC diffusion media. J Electrochem Soc 2007;154:B1295.
[35] Gurau V, Bluemle MJ, De Castro ES, Tsou Y-M, Mann JA, Zawodzinski Jr TA. Characterization of transport properties in gas diffusion layers for proton exchange membrane fuel cells. J Power Sources 2006;160:1156.
[36] Wang XL, Zhang HM, Zhang JL, Xu HF, Tian ZQ, Chen J, et al. Micro-porous layer with composite carbon black for PEM fuel cells. Electrochim Acta 2006;51:4909.
[37] Tang H, Wang S, Pan M, Yuan R. Porosity-graded microporous layers for polymer electrolyte membrane fuel cells. J Power Sources 2007;166:41.
[38] Park S, Lee J-W, Popov BN. Effect of PTFE content in microporous layer on water management in PEM fuel cells. J Power Sources 2008;177:457.
[39] Nakajima H, Konomi T, Kitahara T. Direct water balance analysis on a polymer electrolyte fuel cell (PEFC): effects of hydrophobic treatment and microporous layer addition to the gas diffusion layer of PEFC on its performance during a simulated start-up operation. J Power Sources 2007; 171:457.
[40] Weber A, Newman J. Effects of microporous layers in polymer electrolyte fuel cells. J Electrochem Soc 2005;152:A677.
[41] Ihonen J, Mikkola M, Lindbergh G. Flooding of gas diffusion backing in PEFCs. J Electrochem Soc 2004;151:A1152.
[42] Moreira J, Sebastian PJ, Ocampo AL, Castellanos RH, Cano U, Salazar MD. Dependence of PEM fuel cell performance on the configuration of the gas diffusion electrodes. J New Mater Electrochem Syst 2002;5:173.
[43] Johnson WB, Liu W. Using AC impedance to characterize gas diffusion media in PEM fuel cells. High temperature materials. In: Singhal SC, editor. The electrochemical society

proceedings series, PV 2002-5, Pennington, NJ, 2002. p. 132.
[44] Dong Q, Mench MM, Cleghorn S, Beuscher U. Distributed performance of polymer electrolyte fuel cells under low-humidity conditions. J Electrochem Soc 2005;152:A2114.
[45] Bevers D, Rogers R, von Bradke M. Examination of the influence of PTFE coating on the properties of carbon paper in polymer electrolyte fuel cells. J Power Sources 1996;63:193.
[46] Mathias M, Roth K, Flemin J, Lehnert W. In: Vielstich W, Gasteiger HA, Lamm A, editors. Diffusion media materials and characterization. Handbook of fuel cells—fundamentals, technology and applications, vol. 3, 2003. p. 517 [chapter 42].
[47] Kowal JJ, Turhan A, Heller K, Brenizer J, Mench MM. Liquid water storage, distribution and removal from diffusion media in PEFCs. J Electrochem Soc 2006;153:A1971.
[48] Kim S, Mench MM. Physical degradation of membrane electrode assemblies undergoing freeze–thaw cycling: microstructure effects. J Power Sources 2007;174:206.
[49] Borup R, Davey J, Wood D, Garzon F, Inbody M. PEM fuel cell durability. DOE hydrogen program report, VII.I.3, 2005. p. 1039.
[50] Springer TE, Zawodzinski TA, Wilson MS, Gottesfeld S. Characterization of polymer electrolyte fuel cells using AC impedance spectroscopy. J Electrochem Soc 1996;143:587.
[51] Lefebvre MC, Martin RB, Pickup PG. Characterization of ionic conductivity profiles within proton exchange membrane fuel cell gas diffusion electrodes by impedance spectroscopy. Electrochem Solid-State Lett 1999;2:259.
[52] Li G, Pickup PG. Ionic conductivity of PEMFC electrodes. J Electrochem Soc 2003;150:C745.